AERODYNAMICS OF WIND TURBINES

author:	ŠKORPÍK, Jiří – LinkedIn.com/in/jiri-skorpik
issue date:	January 2023; January 2025 (2nd ed.)
title:	Aerodynamics of wind turbines
proceedings:	*turbomachinery.education*
provenance:	Brno (Czech Republic)
email:	skorpik.jiri@email.cz

Classification of wind turbines according to principle of transformation of kinetic energy of wind into work

HAWT

VAWT

Turbomachine

Drag

According to the orientation of the axis of rotation, wind turbines are classified as horizontal axis wind turbine (HAWT) and vertical axis wind turbine (VAWT). Horizontal axis rotating turbines operate on the principle of the turbomachine in which the air does the work as it flows through the rotor blade passages, see Figure 1a. Vertical axis turbines operate on the principle of variable blade drag during a single rotation, so that, given the same wind direction, they provide different drag at different phases of the rotor rotation, see Figure 1b.
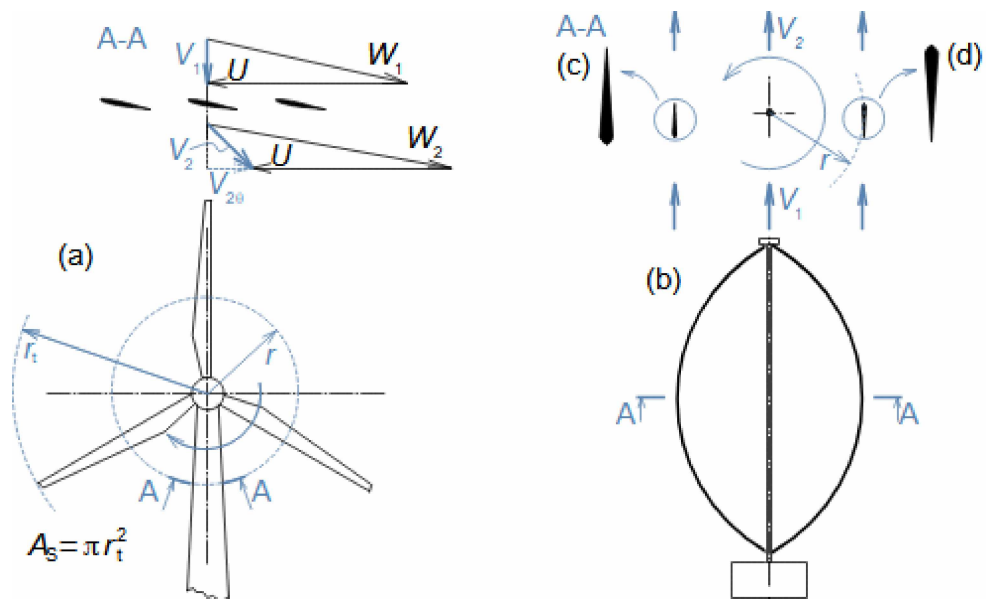
1: Basic types of wind turbine rotors

(a) frontal view of HAWT and cylindrical section A-A of its blade cascade; (b) frontal view of VAWT and section A-A of its rotor (in picture is so-called Darrieus wind turbine, but there are other VAWT types). (c), (d) detail of blade orientation changes and their aerodynamic drag as rotor rotates - in position (c), blade has more drag than in position (d), thus creating moment of force on rotor that causes turbine to rotate. A_S [m^2] rotor swept area; r [m] rotor radius under investigation; r_t [m] tip radius; U [m·s^{-1}] blade speed at radius under investigation; V [m·s^{-1}] absolute airflow velocity; V_θ [m·s^{-1}] tangential component of absolute velocity; W [m·s^{-1}] relative airflow velocity. Index $_1$ indicates the condition in front of the rotor, index $_2$ behind the rotor.

Turbines with the vertical axis of rotation have some advantages (mainly they are not dependent on the wind direction and are able to process the energy of wind gusts), but the dominant type used are horizontal axis turbines, which can have significantly more power and are more efficient - that is what this article is about.

Aerodynamic coefficients of wind turbines

The aerodynamic quantities of wind turbine rotors provide information for design, rotor calculation and rotor loading. Wind turbine aerodynamic quantities include the axial and angular induction coefficients, which describe the changes in velocity in front of and behind the rotor, and the power and thrust coefficients, which describe the energy and force loads on the rotor.

Axial induction coefficient

Stream tube

Miller et al., 1972

The axial induction coefficient a, defined by Formula 2, quantifies the relationship between the wind speed far ahead of the rotor and at the rotor inlet. The air velocity in front of the rotor V_1 is less than the wind speed in the unaffected region in front of the wind turbine V_0. This is due to the formation of a gradually widening tube channel of the rotor, which is formed by the ambient airflow bypassing the slowed air behind the rotor, see Figure 2. This channel is called a stream tube. The axial induction coefficient and velocity V_1 varies along the radius of the blade. The exact velocity distribution in the rotor stream tube is given in [Miller et al., 1972, p. 1261].

$$a = \frac{V_0 - V_1}{V_0}$$
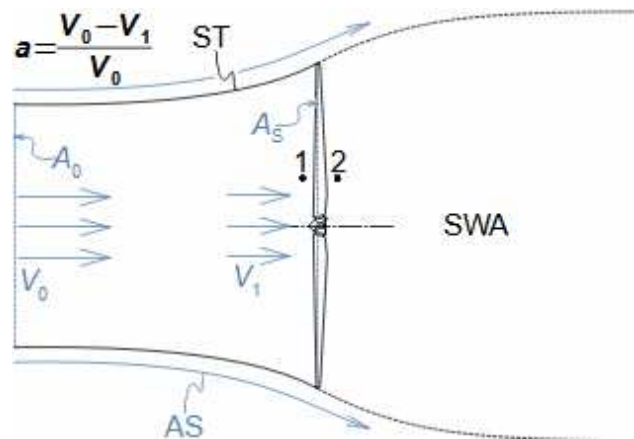
2: Axial induction coefficient of wind turbine

ST-stream tube of rotor; SWA-slowed wind area; AS-ambient stream. A [m^2] flow area; a [1] Axial induction coefficient. The index $_0$ indicates the inlet condition of the stream tube respectively wind speed.

Angular induction coefficient

Helical vortex

The angular induction coefficient a', defined by Formula 3, quantifies the relationship between the helical vortex behind the rotor and the turbine rotational speed. Since a wind turbine is a machine without stator blades, there must necessarily be a helical vortex behind the rotor. The direction of air flow in this vortex is opposite to the direction of rotation of the rotor.

$$a' = \frac{-V_{2\theta}}{2U} = \frac{-\Omega}{2\omega}$$

3: Angular induction coefficient of wind turbine

a' [1] angular induction coefficient; Ω [rad · s^{-1}] angular velocity of healical vortex behind rotor; ω [rad · s^{-1}] angular velocity of rotor. The negative sign in the numerator negates the negative value of the velocity $V_{2\theta}$ respectively the angular velocity of the vortex behind the turbine Ω, which are negative (directed against the positive sense of the tangential direction).

Power coefficient

Thrust coefficient

Part of the kinetic energy of the air flowing through the rotor is transformed into work, respectively power in the form of rotor torque. In addition, the air flow acts in the direction of the flow on the turbine with a thrust in the same way that wind acts on trees, houses and other objects. Quantification of the power and thrust of the wind turbine is done using the power C_P and rotor thrust coefficient C_T. The power coefficient is defined as the power transmitted by the wind to the turbine to the kinetic power of the wind flowing through the same area as the rotor swept area, see Equation 4a. The thrust coefficient is defined as the ratio of the force acting on the rotor in the direction of the axis of rotation (thrust) from the wind flow to the force that would be caused by the dynamic wind pressure on the rotor swept area, see Equation 4a. It is necessary to distinguish between the power and thrust coefficients for the whole rotor and the local one at the radius under investigation, see Equation 4b.

(a)
$$C_P = \frac{P_i}{P_{wind}}; \qquad P_{wind} = \frac{1}{2}\rho V_0^3 \cdot A_S$$
$$C_T = \frac{T}{p_d \cdot A_S}; \qquad p_d = \frac{1}{2}\rho V_0^2$$

(b)
$$C_P = \frac{dP_i}{dP_{wind}}; \qquad dP_{wind} = \frac{1}{2}\rho V_0^3 \cdot dA_S$$
$$C_T = \frac{dT}{p_d \cdot dA_S}; \qquad dA_S = 2\pi r\, dr$$

4: Power and thrust coefficient of wind turbine

(a) parameters for whole rotor; (b) local value of coefficient. C_P [1] power coefficient; C_T [1] thrust coefficient; P_i [W] wind power transferred to wind turbine rotor; P_{wind} [W] kinetic wind power; P_d [Pa] dynamic wind pressure; T [N] thrust on rotor. ρ [kg·m^{-3}] density of air. The equation for the wind kinetic power P_{wind} is derived in Appendix 5.

Comparison of ideal and actual wind turbine rotor

The parameters of an ideal wind turbine rotor are referred to as the Betz limit. Actual rotors cannot achieve these limit due to losses that necessarily occur during energy transformations.

Betz limit

Tyagi and Schmitz, 2025

The ideal rotor theory is used to understand the energy transformation in the wind turbine and to determine the ideal values of the axial, angular, power and thrust coefficients. Most often, the ideal rotor is defined as being exactly in the middle of the stream tube, respectively, the rotor swept area is as large as the mean flow area of the stream tube; the flow through the stream tube is lossless; the distribution of the axial velocity component is uniform, i.e., constant at each point of one axial section; and the velocity at the exit of the stream tube has only an axial direction. Under these assumptions, the values of the axial, angular, power and thrust coefficients can be determined, see Table 5. The value of the power coefficient of an ideal rotor is called the Betz limit.

| a	a'	$C_{P,\,max}$ ($C_{P,\,Betz}$)	C_T
1/3	0	16/27	8/9

5: Parameters of ideal wind turbine rotor

a, a', C_P, C_T [1]. The derivation of the values is shown in Appendix 6. For a different derivation procedure, see [Tyagi and Schmitz, 2025].

Rotational speed

Angular induction coefficient

Table 5 shows that the ideal rotor have an infinitely high rotational speed ($N{\to}\infty$) so that the ratio of the tangential component of the absolute velocity $V_{2\theta}$ and the blade speed U is zero ($a'{=}0$). For these reasons, actual wind turbines have a non-zero angular induction coefficient corresponding to Euler work at a given blade radius.

Losses

Power coefficient

Tip speed ratio

Albert Betz

Actual wind turbines cannot achieve such a high power coefficient value as $C_{P,Betz}$ due to the losses that occur when air flows through the stream tube of the rotor. The magnitude of the losses depends mainly on the number of blades, wind speed, rotor diameter and rotor speed. The rotor diameter and its speed are characterized by the blade speed at the tips U_t. The German aerodynamicist Albert Betz, (1885-1968), while examining measured data of wind turbine rotors, found that the turbine rotor losses vary with the magnitude of the ratio of the blade speed U_t to the wind speed V_0, which he called tip speed ratio λ. Figure 6 plots the power coefficient of an actual two-bladed wind turbine, with the losses corresponding to the difference between $C_{P,Betz}$ (for $\lambda{\to}\infty$) and the actual C_P value. The tip speed ratio at which the turbine reaches the maximum power coefficient value is referred to as the optimum.
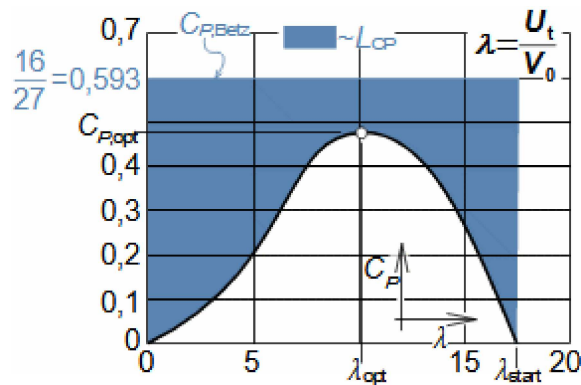
6: Power coefficient of wind rotor and losses according to Betz

L_{CP} [1] power coefficient losses; U_t [m·s^{-1}] blade speed at blade tip; λ [1] tip speed ratio; λ_{start} [1] tip speed ratio at which wind turbine is able to run independently. The index $_{opt}$ indicates the optimum parameters. Data from [Hau, 2006, p. 98].

Power coefficient
Tip speed ratio

The value of the maximum or optimum rotor power coefficient $C_{P,\,opt}$ depends mainly on the number of blades. It only reaches this value at a particular value of the tip speed ratio, referred to as λ_{opt}. The value of λ_{opt} depends not only on the number of blades but also on the shapes of the blade profiles, see Problem 3. Table 7 shows the usual parameters for wind turbine rotors - full C_P-λ curves for different blade numbers are given in [Hau, 2006, p. 98].

Z	1	2	3
λ_{opt}	~15,5	~10,1	~5,75
$C_{P,\,opt}$	~0,42	~0,48	~0,455

**7:** Typical parameters of wind turbine rotors
Data from [Hau, 2006, p. 98]

Helical vortex loss

The dominant loss is the kinetic energy loss of the helical vortex behind the turbine. The absolute value of $V_{2\theta}$, according to the Euler equation for the work of a turbomachine, for the same Euler work decreases with blade speed, therefore the loss in kinetic energy of the vortex increases with decreasing rotational speed. The vortex loss behind the turbine is manifested by the value of the angular induction coefficient a' not being equal to zero as in an ideal rotor.

Profile loss
Flow separation
Vortex generator

Profile losses are caused by the air flow around the blade and are reflected in the profile drag, more about profile losses is in the article Aerodynamics of airfoils [Škorpík, 2022]. A typical problem with wind turbine blades is the small Reynolds number at the blade root and hence the low turbulence of the flow. This also implies an increased sensitivity to flow separation. This is avoided, for example, by installing vortex generators, see Figure 8. Vortex generators stabilise the boundary layer even at lower than optimum wind velocities and are therefore most commonly used in onshore turbines where wind velocities are lower.
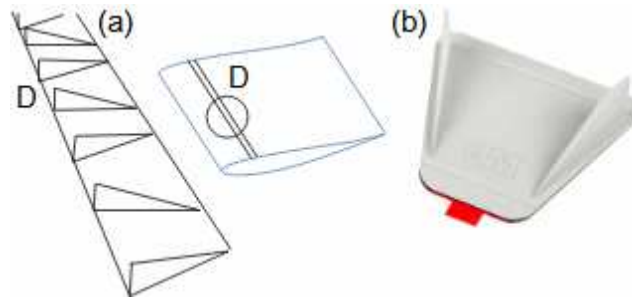
8: Vortex generator of wind turbine blades

(a) detail of vortex generator on pressure side of blade; (b) vortex generator from 3M with adhesive surface (photo 3m.com), which can be used to retrofit turbine blade (for example, when using turbine in location with lower wind speed than it was designed for) - note profile of vortex generator fins.

Tip clearence losses

Tip vortex

Tip clearance losses are losses occurring outside the profile part of the blades. For foot blades it is affected by the flow around the power plant nacelle. In the case of tips, it is mainly a loss by flow overflow from the pressure side of the blade to the suction side of the blade [Wilson et al., 1976, p. 32], so that a tip vortex is formed, which further promotes the formation of vortices along the length of the blade as in the case of aircraft wings [Abbott and Doenhoff, 1959, p. 9], so it is prevented in similar ways as in the case of wings.

Tip vane

Shroud

Tip clearence losses can be reduced by bending the tips of the blades (tip vane) [Hau, 2006, p. 127]. For small wind turbines, a shroud can be used [Hansen, 2008, p. 41] (fixed or static, not connected to blade tips). The shroud subsequently increases the power coefficient of the turbine also by increasing the mass flow of air through the rotor as the tip clearance losses decrease.

Unsteady aerodynamics effects

Velocity profile

Blade aeroelasticity

Unsteady flow

Monopile

In addition to these losses, the rotor performance is affected by unsteady aerodynamic effects, i.e. effects that are variable during the turbine rotation. These include the effect of blade aeroelasticity, including blade untwisting. Long blades already exhibit a different wind speed profile between the highest and lowest blade position, which causes unequal loading on the turbine during a single rotation. This unequal load can cause the entire turbine and consequently the power plant to vibrate and be damaged or destroyed - this must be prevented by the power plant control system. The steady flow through the rotor is also affected by turbulence and vortices behind the turbine, or unsteady airflow (wind gusts). The influence of the monopile is also alternating. For more on these issues, see for example [Hansen, 2006, p. 85], [Manwell et al., 2002, p. 134].

Thrust coefficient

Theorem of momentum
   change

The thrust coefficient equation, derived from the theorem of momentum change (Equation 9a), aligns with experimental results up to $a \approx 1/3$, behind which stream tube collapse increases the thrust coefficient (Figure 9c). While for most turbines the maximum value of the axial coefficient a does not exceed 0,6 [Sharpe, 1990]. According to [Anderson, 1980], the collapse occurs at $a = 0,3262$ and he proposed to approximate the measured data by the straight line defined by Equation 9b, but there are other approximations, see [Wilson et al., 1976, p. 49], [Liew et al., 2024].
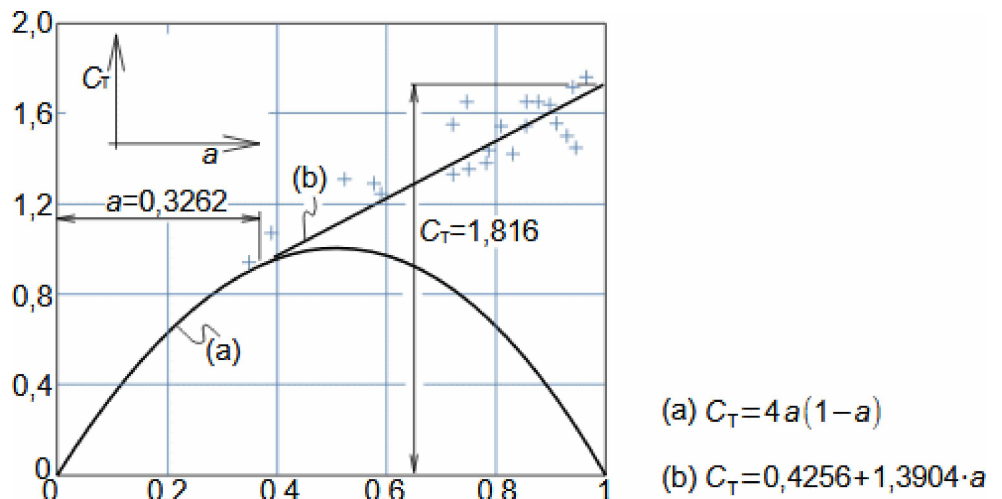
9: Thrust coefficient of wind turbine rotor

(a) equation derived for ideal rotor; (b) approximation of measured values of rotor thrust coefficient starting at $a = 0,3262$; Axial induction coefficient a corresponds to mean value along the length of blades. The derivation of equation (a) is shown in Appendix 7.

Calculation of wind turbine blade shape using aerodynamic coefficients

BEM

Airfoil

The design of the blade is carried out by analytical 2D calculation, i.e. dividing the blade into elementary stages – Blade element method (BEM), see Figure 10. The design is based on an initial estimate of the axial and angular induction coefficient values at the radius under investigation. From these predictions, the velocities in the velocity triangles, the chord length, the stagger angle and the element loading can be calculated using airfoil theory, see the article Aerodynamics of airfoils [Škorpík, 2022]. From there, the local values of the power and drag coefficients can be determined. Verification of the accuracy of the estimation of the axial and angular induction coefficient values at the radius under investigation can be done using the energy and force balance of the blade element being calculated. The total power of the turbine is then the sum of the powers of all blade elements.

Blade profile

Camber of flow

Angle of attack

The basis for the design of the blade calculation is the selection of a suitable blade profile. In particular, the profile must meet the aerodynamic requirements of the profile at the radius under investigation. For example, according to [Stiesdal, 1999], NACA 63 series profiles are suitable for wind turbines. A suitably designed profile will provide the required camber of flow (Figure 12) and therefore work at a given blade radius. This can be influenced mainly by the angle of attack or rotational speed, respectively by the designed tip speed ratio with the magnitude of which the required camber of flow decreases, see Problem 3. The type of profile is varied along the length of the blade to achieve the most optimal aerodynamic and strength properties of the blade. Very thin profiles tend to be used at the tip with a maximum profile thickness to chord ratio of about 0,2, but 0,4 at the root where the blade must be thicker for strength reasons [Hansen, 2008, p. 58]. The sensitivity of dust adhesion on the profile surface and wear are also taken into account, which are determined by the velocity distribution along the profile respectively the profile pressure coefficient. The selection of the profile is also influenced by the noise hygiene requirements of the location.

2D calculation

Chord

Stagger angle

In the 2D calculation of the elementary stage of the wind turbine, we expect that different profile chord length c and stagger angle γ will result for each blade radius under investigation, see Figure 10.
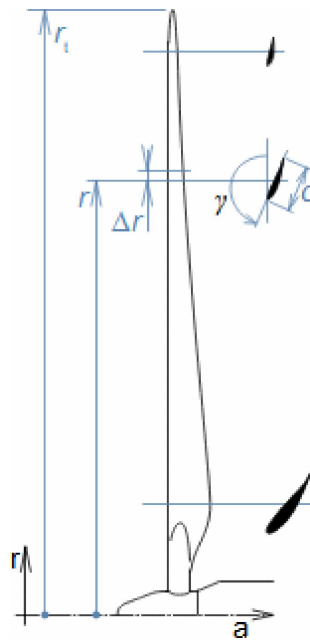
10: Elementary stage of wind turbine

c [m] chord length; γ [°] stagger angle of profile in cascade; Δr [m] height of blade element.

Straight blade

Wind power plant
  Smith-Putnam

Some wind turbine rotors have straight blades. In this case, the optimum profile parameters are achieved at only one radius, usually the mean square radius. The reasons for building such blades are technological. For example, for blades made of metal or wood, respectively, material that cannot be cold-formed into the necessary complex shapes or only very hard at higher cost. For example, the first 1 MW wind turbine in 1941 (see Figure 11) had steel straight blades because the idea was to minimize manufacturing costs [Hau, 2006]. On the other hand, such a simple blade shape obviously leads to higher aerodynamic losses and noise.


11: Wind power plant Smith-Putnam

The Smith-Putnam Wind Power Plant was designed to keep production costs as low as possible. The straight blades were of conventional ribbed design. The inner ribs of the blades were made of steel and the outer steel casing was made of stainless steel. The blades were 20 m long and weighed 8 tonnes each. The rotor diameter was 53,3 m with a rated power of 1 250 kW.

Stagger angle

Axial induction
  coefficient

Angular induction
  coefficient

Mean aerodynamic
  velocity

Using the estimated values of the axial and angular induction coefficients and the optimum value of the tip speed ratio, the velocity angles, in particular the angle of mean aerodynamic velocity W_m, can be calculated (according to Formula 12c). The angle of attack of the mean aerodynamic velocity corresponds to the optimal angle of attack of the blade airfoil and for the proposed Reynolds number. From these data, the stagger angle of the profile γ in the cascade at the investigated radius can also be calculated, see Figure 12 and the solution procedure of Problem 1.
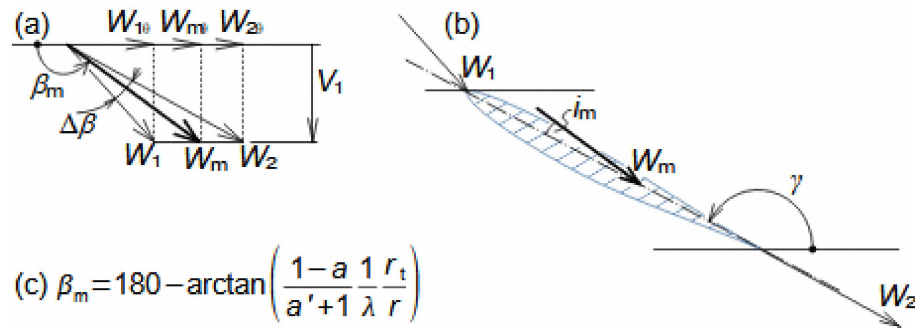
12: Calculation of blade angles on radius under investigation

W_m [m·s^{-1}] mean aerodynamic velocity; β_m [°] angle of mean aerodynamic velocity; $\Delta\beta$ [°] camber of flow; i_m [°] angle of attack of mean aerodynamic velocity (angle between mean aerodynamic velocity and chord). The index $_m$ indicates the mean aerodynamic velocity. The derivation of this formula is shown in Appendix 8.

Chord

    If the basic profile angles are determined, the chord length can be calculated for the proposed Reynolds number value. However, such a calculation already requires knowledge of the wind speed for which the rotor is calculated, see Problem 2.

Blade root

Tip clearence loss

    The calculated length of the chord increases to an extreme with decreasing rotor radius. For this reason, the length of the chord is corrected in this region, giving priority to the strength and weight of the blade. Due to the low power gain in the central region of the rotor relative to the area of the entire rotor, the power loss due to the shortening of the chord is not significant. Aerodynamic elements are usually provided at the tip of the blade to reduce the tip clearence losses.

Force on blade

    The force on the blade element at the investigated radius r from the air flow can be calculated with the lift and drag of the airfoil, see the article Aerodynamics of profile cascades and Figure 13. An example of calculating the force on the blade element is shown in Problem 2.
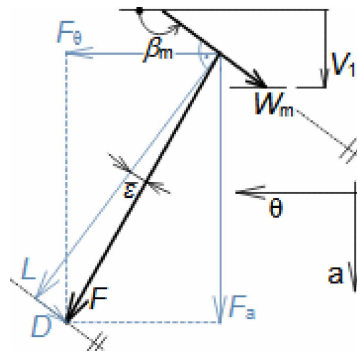
13: Decomposition of force acting on blade on radius under investigation

θ-tangential direction; a-axial direction (axial). D [N] drag; F [N] force acting on blade element from airflow; L [N] lift; ε^- [°] glide angle.

Energy balance

Power coefficient

Axial induction coefficient

Angular induction coefficient

     The accuracy of the estimation of the axial and angular induction coefficients can be verified from the energy balance of the local values of the power coefficient at the investigated radius, which can be calculated in two ways. Firstly, from the tangential force F_θ, respectively the torque from this force (Eq. 14a), and secondly, from the Euler turbine equation (Eq. 14b). The two values must be equal (Eq. 14c), see Problem 3.

$$\text{(a) } C_{P,EW} = \frac{w_E \, d\dot{m}}{\frac{1}{2}\rho V_0^3 dA_S} = 4a'(1-a)\lambda^2\left(\frac{r}{r_t}\right)^2 \qquad \text{(b) } C_{P,AT} = \frac{Z \cdot F_\theta \cdot \lambda}{\rho V_0^2 \pi \cdot r_t}$$

$$\text{(c) } C_{P,EW} = C_{P,AT} = C_P$$

14: Power coefficient of wind turbine elementary stage

m [kg·s^{-1}] mass flow; w_E [kg·s^{-1}] Euler work on investigated radius. (a) power coefficient according to Euler work definition; (b) power coefficient according to airfoil theory; (c) energy balance condition. The derivation of the equations is shown in Appendix 9.

Force balance

Thrust coefficient

     Simultaneously with the energy balance (Eq. 14c) the force balance for the thrust coefficient must be valid. The local values of thrust coefficient can be calculated in two ways. First, using the momentum change theorem (Eq. 15a), and second, using the airfoil theory, respectively from the force F_a (Eq. 15b). The two values must be equal (Eq. 15c), see Problem 3.

$$\text{(a) } C_{T,TM} = 4a(1-a) \qquad \text{(b) } C_{T,AT} = \frac{Z \cdot F_a}{p_d \cdot 2\pi r} \qquad \text{(c) } C_{T,TM} = C_{T,AT} = C_T$$

15: Thrust coefficient of wind turbine blade element

(a) thrust coefficient derived from Theorem of momentum change - formula is already shown in Appendix 7 and is identical to Formula 9 and its validity is confirmed approximately only up to value $a=1/3$; (b) thrust coefficient according to airfoil theory; (c) force balance condition. The derivation of equation (b) is shown in Appendix 10.

Prandtl coeffcient

Camber of flow

Tip clearence loss

     The equality defined by Eq. 14c is based on the assumption that the Euler work w_E is the same over the entire radius under investigation and corresponds to the velocity triangle, respectively the camber of flow in the vicinity of the blades. In reality, the camber of flow varies slightly around the circumference, being largest around the blades and smallest in the axis of the blade passage. The difference increases as the number of blades decreases and near the blade tips, where the effect of tip clearence losses and the radial component of the flow velocity are significant. For this reason, Prandtl proposed to correct the value of Euler work using the C_F factor, see Eq. 16.

(a) $C_{P,EW}$; $C_F = C_{P,AT} = C_P$ (b) $C_F = \dfrac{2}{\pi} \arccos \dfrac{1}{e^f}$; $f = \dfrac{Z}{2} \dfrac{r_t - r}{r \cdot \sin \beta_m}$

16: Prandtl correction of power coefficient

(a) condition for correct design of axial and angular induction coefficient values with Pradtl correction; (b) Prandtl coefficient. C_F [1] Prandtl coefficient.

Hansen, 2008

The product $w_E \cdot C_F$ represents the mean value of Euler work on the investigated radius. The Prandtl coefficient C_F and was originally derived for propellers, but is still used in wind turbine calculations today [Wilson et al., 1976], [Hansen, 2008, p. 52]. Those authors recommend correcting the values of the thrust coefficient in this way, but as Fig. 9 shows, in the region up to about $a=1/3$ its mean value corresponds to Formula 9a without corrections – from this value other types of corrections are used [Hansen, 2008, p. 53]. Fig. 17 shows the results of the wind turbine blade calculation from Problems 1, 2 and 3 with the Prandtl correction.
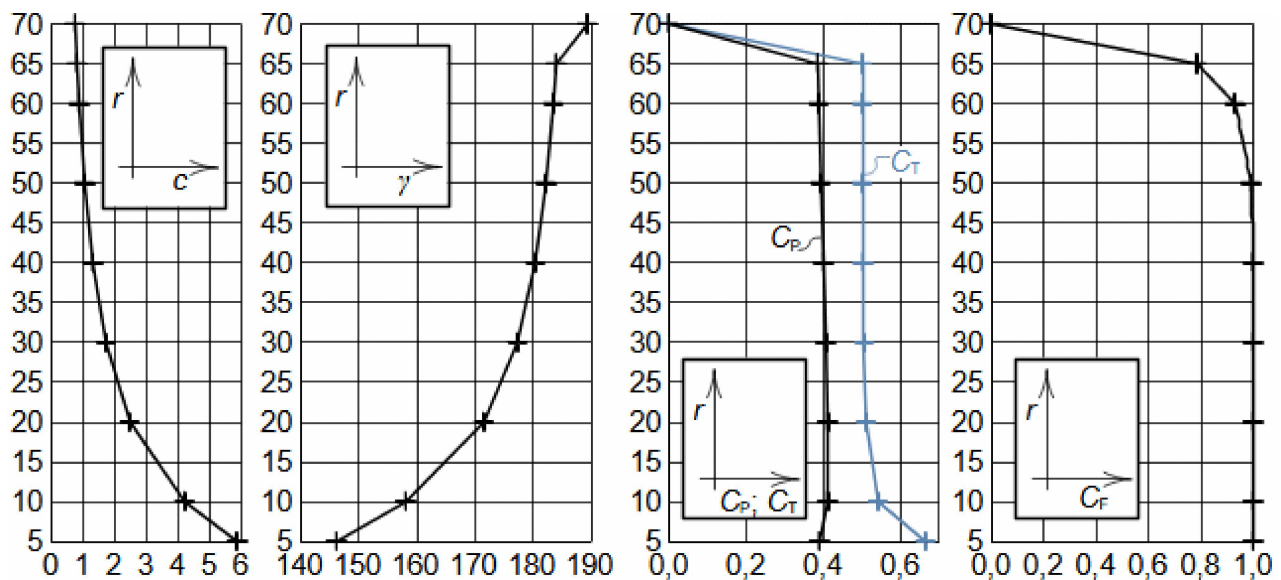
17: Wind turbine rotor blade parameters given in Problems 1, 2 and 3 with Prandtl correction

Parameters are calculated for the case when C_L, C_D and i_m are constant. r [m]; c [m]; γ [m]; C_P, C_T [1]; C_F [1]. The data for the construction of the plots are shown in Appendix 11.

Power characteristics of wind power plant

The usual power characteristic of wind power plants is the dependence of their power P on the wind speed V_0 for the operating rotational speed, see Figure 19. This characteristic can be constructed from the dimensionless wind turbine characteristic C_P-λ [Manwell et al, 2002, p. 129] or, more precisely, by calculating the wind turbine rotor power for each wind speed (see Problem 4 for the calculation of the power for the optimal wind speed) and simultaneously accounting for losses in the mechanisms, the electrical generator, and the own power consumption of power plant.

Wind speed

Start

Shutdown

Nominal power

A wind power plant is only able to generate power within a certain interval of wind velocities. Thus, there is a starting wind speed (the minimum wind speed at which the power plant operates) and a shutdown wind speed (the maximum wind speed allowed). When a wind turbine starts, its output increases with increasing wind speed up to its nominal power or installed power, which is given by the maximum power output of the generator. From the nominal wind speed the power of the wind turbine is maintained at a constant value even when the wind speed increases.

Operation of wind power plants

The control of the wind power plant responds to changes in wind speed with respect to the power characteristics of the wind power plant and its safety. Wind turbine control starts with the start of the turbine and can be done in four basic ways, namely stall control, turning of the blades, rotational speed change and yaw control.

Start

Torque

The regulation of a wind turbine starts with the start of the wind turbine, which is usually not enough to simply unbraking the rotor. As the number of blades decreases, the operating rotational speed decreases and therefore the starting torque increases. So turbines with fewer blades to start need an impulse to turn the rotor, either through the generator or by turning the blades to non-optimal angles designed for a rotating rotor.

Stall control

Asynchronous generator

Aerodynamic brake

Stall control is a simple way to keep the wind turbine rotational speed within the required range. It is used in the case where the wind turbine drives an asynchronous generator, which increases its rotational speed with increasing power, see Figure 18a. This is because as the rotational speed increases, the forces acting on the blade also increase. These forces are used to extend the aerodynamic brakes at the blade tips (Figure 18b) or along the blades at nominal rotational speeds - one possible mechanism for the aerodynamic brake is shown in [Miller et al., 1972, p. 1255]. At the rotational speed of the maximum power output $P_{shutdown}$, the turbine will stop because the wind speed has already reached a level where the aerodynamic brakes are no longer able to effectively control the turbine rotational speed.
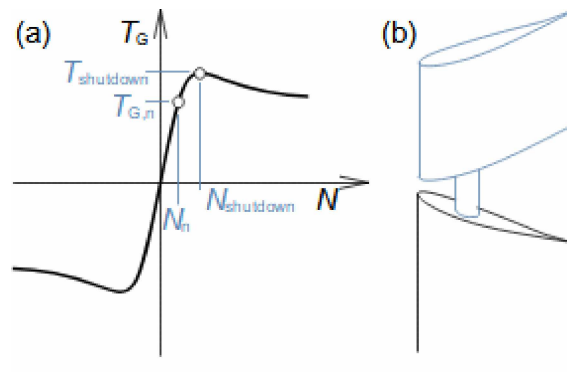
18: Power characteristics of asynchronous generator and aerodynamic brake of wind turbine

(a) power characteristic of asynchronous generator; (b) extendable-turn aerodynamic brake on blade tip in active state. T [N·m] torque; N [s^{-1}] rotational speed. The index $_{shutdown}$ indicates the condition when the wind turbine must be shutdown by the brake; the index $_G$ indicates the generator; the index $_n$ indicates the nominal parameters.

Angle of attack

The aerodynamic brake is not the only control element in the connection of a wind turbine to an asynchronous generator. As the rotational speed and velocities change, the angle of attack i_m also changes, increasing the profile losses and reducing the power output.

_____

Turnable blades

Angle of attack

The power output of a wind turbine can also be controlled by turning the blades using a mechanism in the rotor hub. For power outputs smaller than $P_{e,n}$ (Figure 19), the optimum blade angle of attack i_m is maintained by blade turning. Conversely, when $P_{e,n}$ power is reached, the blades are rotated outside the optimum angle of attack so that $P_{e,n}$ power is not exceeded.

Power characteristics

Stall control

The power outputs of wind power plants with rotating blades are higher than those of stall controlled plants, especially at wind velocities higher than optimum, see Figure 19. They also usually have a wider operating wind speed range.
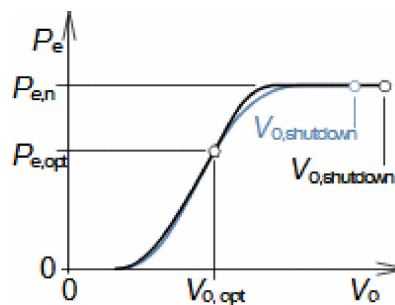
19: Power characteristics of wind power plant with turning blades

blue-wind power plant with stall control; black-wind power plant with blade turning control.

Wind power plant
  Smith-Putnam

The first large wind turbine with automatic blade turning control was the Smith-Putnam wind turbine in 1941, and since then this type of control has become the standard for large wind turbines.

Start

Shutdown

Blade turning is also used during turbine start and shutdown. At start, the angle of attack is set so that the rotor will have the greatest torque. If even this is not enough to spin the turbine, then the rotor must also be spun using a generator running in engine mode. When shutdown occurs, the blades are set to the "flagging" position, i.e. to a position where no lift is generated on the blades and the wind does not spin the turbine.

Rotational speed

Capacity coefficient

The combination of blade turning control with turbine speed variation enables the maximum annual installed capacity of the wind turbine (Capacity coefficient) to be achieved. If the turbine speed can be varied, this means that different generator outputs can be achieved at the same torque depending on the characteristics of the generator. The turbine speed can be varied in steps using a multi-stage gearbox, or continuously using a special gearbox or a multi-frequency generator without gearbox.

Multi-frequency
  generator

Tip speed ratio

Figure 20a shows the *T-N* characteristic of the multi-frequency generator. Note that over a wide range of rotational speeds, the torque of the generator and therefore the turbine remains constant. This allows, to keep the tip Speed Ratio in the optimal region and the turbine operates with a high power coefficient value over a wide range of wind velocities.
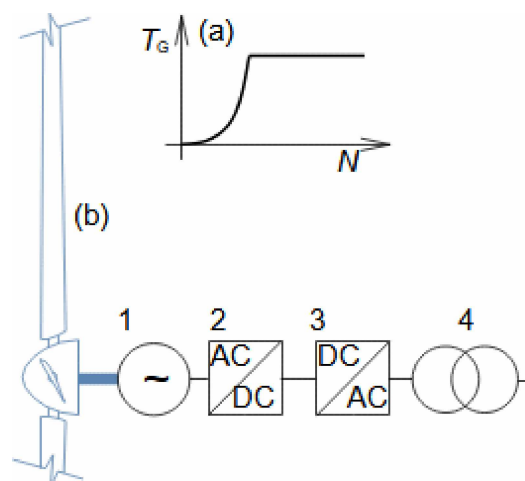
20: Circuit diagram of multi-frequency generator of wind power plant

(a) characteristic of multi-frequency generator; (b) power plants with multi-frequency generator must also include power electronics to change frequency of current. 1-multi-frequency generator; 2-AC to DC converter; 3-DC converter; 4-connection of power plant to transmission grid. AC- alternating current; DC-direct current.

Multi-frequency generators, or generators with gearboxes, are used where there are large fluctuations in wind velocities, respectively in areas where Wind speed is often below the nominal value. These are onshore power plants.

_____

Yaw control

Wind turbine yaw control is performed by turning the turbine around the vertical axis, see <u>Figure 21</u>. It is used to turn the rotor into the wind, or to turn it to a position that prevents the rotor from destroying when the wind exceeds the operational capability of the turbine. Some small turbines also allow turning along the horizontal axis, which acts as an aerodynamic brake.

21: Yaw control wind turbine

Wind turbine blade design

Wind turbine blade design is mostly dependent on the size of the turbine. The smallest turbines have blades made of one piece of material, called solid blades. Larger blades are hollow with a ribbed design inside similar to aircraft wing designs. The blades of large wind turbines are of shell construction with multiple layers and reinforcements, see <u>Figure 22</u>.
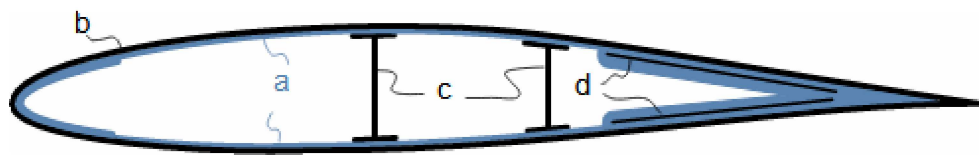
22: Individual layers of shell blade

Shell blade

In the case of the shell design in <u>Figure 22</u>, the inlet and pressure side of the blade are made separately from several layers of fibreglass (<u>Figure 23</u>) - more layers are found at the leading and trailing edges. The two sides are then bonded together by overlapping a common layer of fibreglass. The surface of the blade is cured and smoothed with a covering layer of resin-b. Inside the blade are central reinforcements of light alloys or hardened foam-c. The outlet portions of the suction and pressure sides contain reinforcements-d.

23: Manufacturing wind turbine blades

The picture shows the deposition step of the glass fibre layers before polyester casting at the LM Wind Power factory [Thomsen, 2004].

Untwisting of blades
Blade bending
Humidity

The production of fibreglass blades does not require expensive materials and heat treatment. Blade weights are usually less than 2 tonnes per ten metres of length, with the longest blades being over 100 metres long. The operational problem with long blades is their bending in the axial direction and the danger of the bent blade hitting the monopile. For this reason, wind turbines are not designed for high wind speeds and the rotors have a certain inclination to the horizontal plane so that the blades are further away from the monopile at the bottom. In addition to deformation sensors and vibration sensors, the blades are equipped with lightning arrestors, temperature sensors and other accessories not directly related to their primary function - for example, heating to prevent humidity condensation and frost formation in the blade hollow.

Blade testing
Certification

The blades are tested not only for high-cycle fatigue but also for other weathering resistance, see Figure 24. Finally, the blade must be certified according to IECRE OD-501 (System for Certification to Standards Relating to Equipment for Use in Renewable Energy Applications – Type and Component Certification Scheme - Wind Turbines). This certification can currently only be obtained from about ten certification authorities.

24: Wind turbine blade testing

Testing of blade resistance to lightning strikes at LM Wind Power factory (Netherlands) [Thomsen, 2004].

Service life
Refurbishing

The blades are designed for a service life of approximately 20 years. During this time they must be fully functional without the need for repainting, but even then their surface can be refurbished on site (they do not have to be removed from the wind turbine), see Figure 25.

25: Wind turbine blade after refurbishing its surface - first after 20 years of operation

The 28 m long blade of the Vestas V52 wind turbine.

Problems

Problem 1:

Calculate the basic angles of the rotor blade of a wind turbine with a diameter of 140 m and three blades. Carry out the calculation on a radius of 10 m for NACA profile 63-209. Estimate the axial and angular induction coefficient values only for now. The solution to the problem is shown in Appendix 1.

§1	entry:	r; r_t; Z	§4	proposal:	Re
§2	estimate:	a; a'		read off:	i_m
§3	proposal:	λ	§5	calculation:	γ
	calculation:	β_m			

Symbol descriptions are in Appendix 1.

Problem 2:

Calculate the length of the chord and the forces acting on the rotor blade element from Problem 1. Carry out the calculation for a nominal wind speed of 6,8 m·s⁻¹ and an air density of 1,2 kg·m⁻³. The solution to the problem is shown in Appendix 2.

§1	entry:	ρ; V_0		calculation:	V_1; W_m; c
§2	proposal:	t	§3	read off:	C_L; C_D
	read off:	v; β_m; a		calculation:	L; D; F; ε; F_θ; F_a

Symbol descriptions are in Appendix 2.

Problem 3:

Calculate the power and thrust coefficients in the blade element region of the wind turbine solved in Problem 1 and 2. Also calculate the rotor rotational speed. The solution to the problem is shown in Appendix 3.

§1	read off:	a'; a; λ; r; r_t; Z; F_θ; ρ; V_0; F_a viz Problem 1 a 2
§2	calculation:	$C_{P,EW}$; $C_{P,AT}$; $C_{T,TM}$; p_d; $C_{T,AT}$
§3	comparison:	If the equality in Equation 14c or Equation 15c is not satisfied, then the coefficient values entered in Problem 1 are non-optimal and the calculation must be repeated from Problem 1 with new estimates.
§4	calculation:	N

Symbol descriptions are in Appendix 3.

Problem 4:

Calculate the expected rotor power of the wind turbine from the problem solved in Problems 1, 2 and 3. The final blade parameters are shown in Figure 17. Also calculate the power and thrust coefficient of this rotor. The solution to the problem is shown in Appendix 4.

§1	read off:	r; $C_{P,j}$; $C_{T,j}$; V_0; ρ; p_d	§2	calculation:	P_i; T
	calculation:	$\Delta A_{S,j}$; $\Delta P_{wind,j}$; $\Delta P_{i,j}$; ΔT_j	§3	calculation:	P_{wind}; C_P; C_T

Symbol descriptions are in Appendix 4.

References

ŠKORPÍK, Jiří, 2022, Aerodynamika profilů, *fluid-dynamics.education*, Brno, https://fluid-dynamics.education/aerodynamika-profilu.html.

ABBOTT, Ira, DOENHOFF, Albert, 1959, *Theory of wing sections, including a summary of airfoil data*, Dover publications, inc., New York, ISBN-10:0-486-60586-8.

ANDERSON, M. B., 1980, A vortex-wake analysis of a horizontal axis wind turbine and a comparison with modified blade element theory, *Proceedings of the Third International Symposium on Wind Energy Systems*, Copenhagen, BHRA Fluid Engineering, paper no. H1 357–374.

DIXON, S., HALL, C., 2010, *Fluid Mechanics and Thermodynamics of Turbomachinery*, Elsevier, Oxford, ISBN 978-1-85617-793-1.

HANSEN, Martin, 2008, *Aerodynamics of wind turbines*, Earthscan Ltd., London, ISBN 978-1-84407-438-9.

HAU, Erich, 2006, *Wind Turbines – fundamentals, technologies, Applications, Economics*, Springer, Berlin, Heidelberg, New York, ISBN-10-3-540-24240-6.

LIEW, Jaime, HECK, Kirby, HOWLAND, Michael, 2024, Unified momentum model for rotor aerodynamics across operating regimes, Nature Communications 15, 6658, https://doi.org/10.1038/s41467-024-50756-5.

MANWELL, J.F., MCGOWAN, J.G. and ROGERS A.L., 2002, *Wind Energy Explained – Theory, Design and Application*, John Wiley & Sons Ltd, ISBNS: 0-471-49972-2.

MILLER, Rudolf, HOCHRAINER, A., LÖHNER, K., PETERMANN, H., 1972, *Energietechnik und Kraftmaschinen*, Rowohlt taschenbuch verlag GmbH, Hamburg, ISBN 3-499-19042-7.

SHARPE, D. J., 1990, Wind turbine aerodynamics, *Wind Energy Conversion Systems*, Englewood Cliffs.

STIESDAL, Henrik, 1999, *The wind turbine components and operation*, Bonus Energy A/S, Brande. Dostupné z *http://www.windmission.dk*.

THOMSEN, Troels, 2004, *Reliability of large rotor blades*, AusWIND 2004 in July 28 – 30, Launceston, Tasmania.

TYAGI, Divya, SCHMITZ, Sven, 2025, Glauert's optimum rotor disk revisited – a calculus of variations solution and exact integrals for thrust and bending moment coefficients, *Wind Energy Science*, 10, 451–460, https://doi.org/10.5194/wes-10-451-2025.

WILSON, R., LISSAMAN, P., WALKER, Stel, 1976, *Applied Aerodynamics of Wind Power Machines*, Oregon State University.